

This article was downloaded by: [CDC]

On: 21 February 2012, At: 06:18

Publisher: Taylor & Francis

Informa Ltd Registered in England and Wales Registered Number: 1072954

Registered office: Mortimer House, 37-41 Mortimer Street, London W1T 3JH, UK



Aerosol Science and Technology

Publication details, including instructions for authors and subscription information:

<http://www.tandfonline.com/loi/uast20>

Relationships Between Electrostatic Charging Characteristics, Moisture Content, and Airborne Dust Generation for Subbituminous and Bituminous Coals

Steven J. Page

Available online: 30 Nov 2010

To cite this article: Steven J. Page (2000): Relationships Between Electrostatic Charging Characteristics, Moisture Content, and Airborne Dust Generation for Subbituminous and Bituminous Coals, *Aerosol Science and Technology*, 32:4, 249-267

To link to this article: <http://dx.doi.org/10.1080/027868200303605>

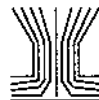
PLEASE SCROLL DOWN FOR ARTICLE

Full terms and conditions of use: <http://www.tandfonline.com/page/terms-and-conditions>

This article may be used for research, teaching, and private study purposes. Any substantial or systematic reproduction, redistribution, reselling, loan, sub-licensing, systematic supply, or distribution in any form to anyone is expressly forbidden.

The publisher does not give any warranty express or implied or make any representation that the contents will be complete or accurate or up to date. The accuracy of any instructions, formulae, and drug doses should be independently verified with primary sources. The publisher shall not be liable for any loss, actions, claims, proceedings, demand, or costs or damages whatsoever or

howsoever caused arising directly or indirectly in connection with or arising out of the use of this material.



Relationships Between Electrostatic Charging Characteristics, Moisture Content, and Airborne Dust Generation for Subbituminous and Bituminous Coals

Steven J. Page

NATIONAL INSTITUTE FOR OCCUPATIONAL SAFETY AND HEALTH
PITTSBURGH RESEARCH LABORATORY
PO BOX 18070
PITTSBURGH, PA 15236

ABSTRACT. Small scale laboratory pulverizing experiments were performed on humidified coal material sieved to size 6.35 mm (0.250 in) and below to eliminate effects due to inherent planes of weakness (cleats or joints). Experimental factors studied include the coal seam proximate analysis constituents, the breakage-induced electrostatic field of airborne dust, and the specific airborne dust generated. Results of these pulverizing experiments show that only coals below 1–2% air dry loss (ADL) moisture content are in a highly charged state after pulverization and that the amount of charging decreases rapidly with increasing ADL up to 1–2%. This appears to have a direct effect on the specific dust generation characteristics of coals. However, each coal may have its own characteristic dust charge and generation signature. Underground dust samples obtained in coal seams with inherent moisture contents ranging from 0.5 to 4.5% suggest that significant particle agglomeration exists for the 0.5% inherent moisture coal but not the coals with moisture > 1.3% inherent moisture, in agreement with the laboratory tests.

INTRODUCTION

Prolonged exposure to airborne respirable coal dust is responsible for the prevalence of Coal Workers' Pneumoconiosis (CWP). Health research studies have identified that the severity of CWP is directly related to the amount of dust exposure and the coal rank (Attfield and Seixas 1995; Attfield and Morring 1992; and Hurley and Maclaren 1987). Since the passage of the 2.0 mg/m³ dust standard (average shift concentration exposure limit) in the Federal Coal Mine

Health and Safety Act of 1969 (U.S. Congress 1969), average dust levels were reduced from over 6 mg/m³ to current levels just under the 2.0 mg/m³ standard (Attfield and Wagner 1992). The National Institute for Occupational Safety and Health (NIOSH) has recently determined through their Coal Worker's X-ray Surveillance Program that coal miners continue to have an elevated risk for CWP under the current 2.0 mg/m³ dust standard and recommended a 1.0 mg/m³ dust standard to

reduce the prevalence of CWP (Criteria for a Recommended Standard 1995). To achieve this goal, coal mine worker dust exposure needs to be notably reduced.

Prior research has identified several relationships between coal seam rank and dust generation. Laboratory coal comminution studies have shown a significantly consistent positive correlation between coal rank and the amount of respirable-sized particles found in the product (Srikanth et al. 1995; Moore and Bise 1984; and Baafi and Ramani 1979). These studies show conclusively that either a grinding or crushing process yield total and respirable dust generation rates (milligrams of dust in product per kilogram of product) which increase with coal rank. Baafi's and Moore's investigations obtained this result by the Hardgrove Grindability Index (HGI) ASTM procedure, whereas Srikanth et al. employed single breakage tests and used a combination of sieve and laser spectrometer analysis to estimate the amounts of minus-15 and minus-7 μm dust in the product. It is important to note that these results were measurements of dust *in the product* and not measurements of airborne dust.

Other research studies of airborne dust generation and coal rank have shown different relationships. The National Coal Board's (NCB) Mining Research Establishment had initially observed discrepancies in airborne dust and the product sizes produced as compared to the breakage processes of the coal (Knight 1958 and Hamilton and Knight 1957). Laboratory shatter (drop test) and tumble breakage tests (friability type test) were conducted on various coal seams mined in Great Britain and showed negative correlations between coal strength (compressive strength) and the product sizes. Although the higher ranked weaker coals (lower compressive strength coals) consistently produced a smaller product size distribution, airborne dust

generation differences were observed between these two breakage processes. A negative airborne dust correlation with coal strength (or positive with coal rank) was observed for the tumble tests, but no airborne dust correlation was observed for the shatter tests. Conclusions drawn were that weaker coals (higher rank coals) had a lower portion of dust in the product dispersed during the shatter breakage tests and that airborne dust generated is somewhat related to the violence upon which the particular coal breaks.

Underground and laboratory studies conducted by the U.S. Bureau of Mines in the late 1980's and early 1990's showed an opposite correlation between coal rank and airborne dust generation as compared to previously established coal rank and in-product size distribution relationships. An underground survey of 20 longwalls operating in 16 different bituminous coal seams throughout the United States indicated that high volatile, low ash coal seams (lower ranked coals) tended to produce more airborne respirable dust (ARD) (Organisak et al. 1992). Additional USBM laboratory work on feeding nine bituminous coals of 4.75 mm \times 5.66 mm (0.187-in \times 0.223-in) size through a small roll crusher with 38.1 mm (1.5-in) diameter rolls spaced 3.18 mm (0.125-in) apart indicated that lower ranked coals, as described by their fuel ratio (fixed carbon/volatile matter), also produced more total airborne dust (Page et al. 1993). Although the general airborne dust and coal rank relationships were similar for the laboratory and underground studies, differences in the correlation of particular coal parameters, such as ash, was believed to be an extraneous variable associated with the inherent weakness of the coal's cleat (or joint) structure. Others have postulated that coal fragmentation from cutting usually occurs along planes of imperfections (cleats or joints) or weaknesses formed by

mineral matter (Stecklein et al. 1982). However, existence of correlations between coal parameters such as volatile matter, ash, fixed carbon, or moisture content and ARD does little to explain the underlying mechanisms responsible for the correlations. Indeed, understanding these mechanisms involved in ARD generation would likely identify new engineering control attributes needed for improving coal mine dust suppression developments.

It has long been known that airborne dust particles can have a significant amount of electrostatic charge (Hopper and Laby 1941; Kunkel 1948; Kunkel 1950; and Dodd 1952) and that this charge can place dusts in varying degrees of agglomeration (Kunkel 1948; Kaya and Hogg 1992). Coal mine worker health and dust control methods are more than likely to be influenced by these charging and agglomeration characteristics. For example, the amount of ARD generated affects worker exposure as well as the type and level of dust controls required. In addition, dust control methods are invariably more effective on the larger sized thoracic component of dust which is also believed to be a health concern. Also, lung deposition was found to increase directly with charging properties of airborne dust (Melandri et al. 1983). The increased prevalence of CWP observed with coal rank may be partly related to the increased dust cloud charging in higher ranked coals as measured by Organiscak and Page (1998). This increased deposition may also be attributed to the higher lung deposition efficiency of agglomerated ultrafine submicron particles as well as to image charging effects within the lung (Yu and Chandra 1978 and Becker et al. 1980).

Kaya and Hogg (1992) state that one would not intuitively expect significant agglomeration of airborne dust in the mine atmosphere at the levels of dust concentrations found even in the most dusty mines.

They also postulate that the observed agglomeration (Polat et al. 1991) occurs immediately at the point of dust generation. Kunkel (1948) concludes that agglomeration will be negligible if the dust cloud density $< 10^6$ particles/cm³ or if the average charge of one sign is well below a thousand electrons per particle. For an 8 μ m coal particle, this particle density would roughly be equal to 350 gm/m³ mass concentration. This level of dust concentration could only be found at the very source of dust generation, as postulated by Kaya and Hogg.

In order to identify some of the factors responsible for airborne total dust generation, NIOSH conducted small scale laboratory pulverizing experiments on humidified coal material sieved to size 6.35 mm (0.250 in) and below to eliminate effects due to inherent planes of weakness (cleats or joints). Experimental factors studied include the coal seam proximate analysis constituents, the electrostatic charge field of airborne dust, and the specific airborne total dust generated. The total dust generated was characterized by measuring the simultaneous penetration through energized and unenergized electrostatic precipitators using both size-classifying impactors and filter cassettes. This report describes the research findings of pulverizing tests on 16 different bituminous coal samples as well as on Pittsburgh seam coal containing varying degrees of ADL moisture. In addition, corroborative data from underground coal mine dust samples is presented.

EXPERIMENTAL DESIGN

Test Facility

The dust generating and sampling chamber shown in Figure 1 consisted of a 0.0283 m³ (1 ft³) plywood box with a removable lid located within a larger chamber. The pul-

verizer used to crush the coal was a 0.25 kW (1/3 hp) disk mill using 10.2 cm (4 in) plates. Feed material loaded into the pulverizer hopper was fed to the plates by an auger. Fresh-generated airborne dust was produced by running the pulverizer for either 45, 30, or 15 s per run prior to the start of dust sampling. Total pulverizing times reflect the total for 2 consecutive runs. Differing pulverizing times were used based upon the quantity of airborne dust being generated to prevent overload of the dust sampling impactor stages. However, since all reported pertinent data is normalized per unit of material pulverized, the results are invariant to the pulverizing time. On the bottom of the sampling chamber, below the pulverizer discharge, was a 25.4 cm (10 in) diameter pan for catching the falling material. Resting on top of the pan was a stainless steel tray with the same dimensions as the inside of the chamber. This tray served to capture airborne dust which

would settle inside the chamber at the same time the total airborne dust samples were being collected. The pulverized material fell through one slot in the lid and a second slot in the tray before impact in the pan. A partial partition was installed in the chamber, as shown, to buffer the dropping volume from the airborne sampling volume. At the end of the test, the material passing through the pulverizer was removed and weighed. The pulverizer, feed and collection hoppers, and dust sampling lines were vacuumed and flushed clean with nitrogen gas. This procedure was followed also for replicate tests of the same coal sample.

Material from both the pan and the tray were saved in sealable plastic bags for proximate analysis. The total material which passed through the pulverizer and collected for each test was analyzed for ash, moisture, volatile matter, and fixed carbon content. Tables 1 and 2 summarize the analysis results for the tests. In Table 2, as-received

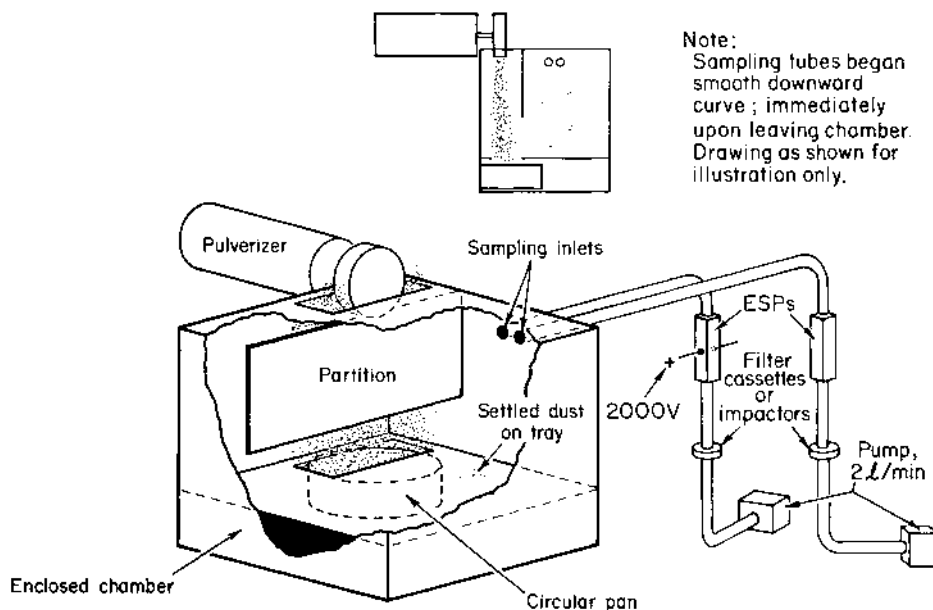


FIGURE 1. Diagram of laboratory pulverization apparatus.

TABLE 1. Proximate analysis of 16 coal samples tested.

Mine	as-determined basis							
	Total Moisture %	Air Dry Loss, %	Inherent Moisture %	Ash, %	Volatile Matter, %	Fixed Carbon, %	MFR, ^a ADL	MFR, Inherent
A	1.7	0.9	0.8	2.2	32.3	64.7	2.3	2.6
B ^b	1.7	1.0	0.7	11.4	19.3	68.7	3.7	5.1
C	6.1	3.7	2.5	6.3	45.1	46.2	0.3	0.4
D	1.5	1.0	0.6	5.3	29.2	65.0	2.3	3.9
E	4.8	2.7	2.1	8.7	41.5	47.7	0.4	0.6
F	2.7	1.3	1.3	14.1	30.8	53.8	1.3	1.3
G	2.1	1.0	1.0	5.8	37.2	56.0	1.5	1.4
H	1.3	0.6	0.6	5.1	32.4	62.0	3.0	3.1
I	1.0	0.6	0.4	31.2	17.5	50.8	4.8	6.8
J	4.5	2.4	2.1	7.9	42.2	47.8	0.5	0.5
K	1.9	1.2	0.8	3.9	30.8	64.5	1.8	2.7
L	1.7	0.9	0.8	25.8	24.7	48.7	2.3	2.4
C	6.3	4.5	1.9	6.4	44.3	47.4	0.2	0.6
A	1.6	1.1	0.5	2.2	32.7	64.6	1.7	4.1
D	1.7	1.3	0.4	5.3	29.1	65.2	1.8	5.2
F	3.0	2.0	1.0	13.9	30.4	54.7	0.9	1.8
I	1.1	0.9	0.3	28.7	18.0	53.0	3.5	11.3
E	5.2	3.8	1.4	8.6	41.8	48.2	0.3	0.8
C	6.5	4.9	1.5	6.2	45.1	47.2	0.2	0.7
A	1.7	1.2	0.5	2.2	33.2	64.1	1.6	3.8
B ^b	1.8	1.4	0.5	11.4	19.6	68.6	2.5	7.8
K	2.1	1.4	0.7	3.7	30.3	65.3	1.5	3.2
M ^b	6.7	5.4	1.2	6.2	38.9	53.7	0.3	1.1
N ^b	8.7	6.8	1.9	22.1	33.7	42.3	0.2	0.6
O ^b	7.8	6.8	1.0	16.7	31.7	50.6	0.2	1.6
P ^b	8.4	6.7	1.7	9.1	39.0	50.2	0.2	0.8
L	2.1	1.5	0.6	28.6	23.8	47.1	1.3	3.4
G	2.5	1.7	0.7	6.0	36.1	57.2	0.9	2.1
J	5.2	4.0	1.2	7.9	42.9	48.0	0.3	0.9
J	4.6	3.3	1.3	7.9	42.3	48.6	0.3	0.9
J	4.7	3.5	1.2	7.5	43.4	47.9	0.3	0.9

^a: MFR defined as fixed carbon/volatile matter/moisture.^b: Samples obtained from longwall run-of-mine material.

analysis was inadvertently performed on the first eight samples without reporting the ADL moisture content. Since there was little difference in the inherent moisture values, the average inherent moisture was used to estimate the ADL content of the total moisture for these samples. Since it was not the purpose of this study to accurately characterize by proximate analysis the coal seam itself, it was not necessary to follow ASTM standard sample preparation

techniques. Rather, it was hoped that variations in proximate analyses between the replicate samples from a given coal seam would manifest themselves in the quantities of airborne total dust generated. ASTM standards (ASTM D3172 1996) for the proximate analysis were used.

The dust which became airborne from dispersion was primarily generated by impact in the collection pan and secondarily as the material fell through the chamber.

TABLE 2. Proximate analysis of humidified Pittsburgh seam coal samples tested.

Test	As-received					As-determined			
	Ash, %	Volatile Matter, %	Fixed Carbon, %	Total Moisture %	Air Dry Loss ^a , %	Inherent Moisture, %	Ash, %	Volatile Matter, %	Fixed Carbon, %
1	5.9	35.1	56.9	2.1	1.2				
2	6.0	35.3	56.5	2.2	1.2				
3	5.6	35.5	55.8	3.2	2.3				
4	5.4	35.6	56.3	2.7	1.8				
5	5.5	35.6	57.0	1.9	0.9				
6	4.9	36.4	56.1	2.6	1.7				
7	5.3	35.6	56.0	3.1	2.2				
8	5.4	35.6	56.3	2.8	1.9				
9				2.6	1.6	1.0	5.5	36.9	56.7
10				2.4	1.4	1.0	5.3	36.3	57.4
11				2.7	1.7	1.0	5.1	36.6	57.3
12				3.8	2.8	1.0	5.3	37.3	56.3
13				2.5	1.6	0.9	5.1	37.0	57.0
14				2.1	1.4	0.7	5.3	37.1	57.0
15				2.3	1.3	1.0	5.1	36.3	57.6
16				2.4	1.3	1.0	5.4	36.9	56.7
17				2.2	1.0	1.1	5.1	36.5	57.3
18				2.2	1.1	1.1	5.3	36.8	56.9
19				2.0	1.1	1.0	5.5	36.7	56.9
20				2.0	0.9	1.0	5.3	36.9	56.8
21				1.9	1.1	0.8	5.4	36.7	57.2
22				3.5	2.7	0.9	5.5	36.3	57.3
23				3.6	2.8	0.8	5.7	36.1	57.4
24				5.8	4.9	0.8	5.4	36.4	57.4
25				4.8	4.1	0.7	5.4	36.5	57.3
26				1.6	0.6	1.0	5.1	36.6	57.4
27				1.5	0.7	0.8	5.7	36.1	57.4
28				1.5	0.5	1.0	5.4	36.2	57.5
29				1.5	0.6	0.9	5.0	36.5	57.6
30				1.7	0.6	1.1	5.2	36.4	57.3
31				1.7	0.7	1.0	5.0	36.3	57.7
32				1.6	0.7	1.0	5.4	36.4	57.3
Average					1.6	0.9	5.3	36.6	57.2
Standard Deviation					1.1	0.1	0.2	0.3	0.3
Coefficient of Variation					73.0%	12.1%	3.8%	0.9%	0.6%

^a Values for the ADL in tests 1–8 are estimated by subtracting the average inherent moisture value from the total moisture.

The airborne total dust was gravimetrically sampled by two 6.35 mm (1/4 in) inside diameter flow lines simultaneously with pumps operating at 2 l/min for a 3 min period, beginning 15 s after end of the pulverization period. Since the sampling did not begin until 15 s after the end of pulver-

ization and given the height of the chamber, particles larger than approximately 20 μm will have settled out of the air before sampling begins. Each flow line contained an identical parallel plate electrostatic precipitator (ESP) of internal dimension 12.7 mm \times 12.7 mm \times 20.3 cm (0.5 in \times 0.5 in \times

8 in) mounted in vertical position to minimize gravitational settling effects. The design is similar to that reported by Johnston (1983) with the fundamental differences that the flow was not split within each ESP and the applied voltage to only one ESP was held constant at 2000 VDC. At this operating voltage no corona discharge was produced within the ESP. As a result, no significant additional particle charging was expected to occur within the ESP. The second ESP had no applied voltage and removed no particulate via electrostatic effects.

The dust penetration output of each ESP was collected gravimetrically in one of two different ways. For the coal samples listed in Table 3 the dust was collected by Model 298 Sierra personal impactors. The impactor stages 1 through 6 (20 μm through 1.55 μm 50% cut point sizes) were used with the < 1.55 μm particle sizes collected on the final filter. For the Pittsburgh coal samples listed in Table 4, the dust was collected by 37 mm Mine Safety Appliance (MSA) filter cassettes. Each test consists of two runs. After the first run the sampling pumps were interchanged and the second run performed so that variations between sampling flow lines would be minimized. The mass sampling precision of the two flow lines using this procedure was determined to be within $\pm 5\%$, based upon fifty replicate baseline tests performed with no applied voltage to the ESP prior to collection of this data set.

Concurrent with the pulverization of the coal samples, electrostatic field measurements were made at a fixed location within the small chamber containing the dust cloud by a Monroe 245 electrostatic field meter. Analog output of the fieldmeter was fed into a DC amplifier to provide an offset voltage sufficient to compensate for negative values of the electrostatic field. The signal was then fed into a second amplifier

to achieve proper calibration at full scale deflection of the fieldmeter over the range of interest. The fieldmeter was rezeroed and the calibration adjusted prior to each test. The output signal was then stored on a data logger for computer averaging to obtain a value proportional to the average dust cloud charge.

Coal Sample Collection and Preparation

Coal samples used for testing were obtained from three source groups: 1) Channel samples were collected from active continuous miner faces at ten coal mines in nine seams from the Eastern and Rocky Mountain provinces of the United States. The Eastern province samples represent coals from both Northern and Southern regions; 2) Pittsburgh coal from NIOSH's Safety Research Coal Mine at the Pittsburgh Research Center (PRC); and 3) Run-of-mine (ROM) coal from five long-wall panels which cut minimal amounts of rock material. Each sample was initially sieved to extract the > 2.82 mm (0.111 in) to < 6.35 mm (0.250 in) size fraction already present in the material. To obtain additional material for the tests, the > 6.35 mm coal was processed through a 1.1 kW double roll crusher and resieved. Rock pieces were intentionally rejected from the prepared samples because rock-generated dust should be treated separately from coal-generated dust due to the likely difference in generation characteristics.

After obtaining the desired size fraction of material to be pulverized, all samples were laid out in shallow pans in a sealed chamber. The chamber was humidified with a vaporizer until saturation at ambient barometric pressure was achieved. A fan within the chamber circulated the humid air at all times. This condition was maintained for an arbitrary time period of several weeks to increase the moisture content

TABLE 3. Dust mass and electrostatic charge generation characteristics of 16 coals tested.

Mine	$M(u)^a$ mg	$M(u) - M(e)^b$ $= M(p)$ mg / mg / kg	Specific Dust mg / kg	Median Size ^c (GSD) exiting ESP's		Average Electric Field, E, Volts / cm	Average Specific Field, E _s , V / cm / mg / kg
				$M(u)$ μm	$M(e)$ μm		
A	3.28	1.06	5.98	7.5 (2.00)	7.0 (1.98)	N/A	N/A
B ^d	1.49	1.29	3.05	7.1 (1.92)	7.8 (1.78)	N/A	N/A
C	3.25	0.54	5.29	5.6 (2.07)	6.0 (2.08)	N/A	N/A
D	1.99	1.26	3.93	6.8 (1.99)	6.8 (1.98)	N/A	N/A
E	5.60	0.66	8.58	6.2 (2.04)	5.7 (1.96)	N/A	N/A
F	1.58	1.24	2.56	7.6 (2.01)	5.3 (1.85)	N/A	N/A
G	1.53	1.27	2.86	7.7 (1.95)	7.6 (2.17)	N/A	N/A
H	3.44	1.27	6.13	6.4 (1.93)	4.8 (1.73)	6.7	1.1
I	1.43	1.12	2.39	7.0 (1.91)	6.0 (1.82)	11.7	4.9
J	4.34	0.80	7.03	6.3 (2.02)	5.6 (1.97)	8.3	1.2
K	2.42	1.18	4.69	7.3 (1.98)	6.6 (2.02)	10.9	2.3
L	1.44	1.21	2.48	7.1 (1.83)	6.1 (1.78)	1.7	0.7
C	6.82	0.75	10.98	7.5 (2.05)	7.0 (2.09)	-12.2	-1.1
A	3.58	0.99	6.47	7.1 (1.83)	7.3 (2.05)	13.9	2.1
D	3.78	1.01	6.76	8.1 (2.02)	7.1 (2.05)	37.8	5.6
F	2.33	1.09	3.73	9.2 (1.94)	8.2 (2.14)	-5.3	-1.4
I	2.27	1.36	5.30	7.6 (1.99)	7.7 (2.00)	N/A	N/A
E	4.47	0.61	10.59	6.3 (2.00)	7.0 (2.05)	-1.1	-0.1
C	3.22	0.40	8.00	5.1 (2.06)	6.0 (2.07)	-10.9	-1.4
A	2.41	0.80	6.55	6.4 (2.01)	7.5 (2.04)	25.0	3.8
B ^d	0.72	0.93	2.12	6.7 (2.00)	7.2 (2.07)	21.8	10.3
K	3.49	1.34	9.81	7.2 (1.93)	7.5 (2.01)	30.1	3.1
M ^d	4.92	1.14	11.47	7.5 (1.93)	7.8 (1.96)	4.9	0.4
N ^d	5.82	0.92	13.17	6.3 (1.89)	6.8 (1.88)	-8.5	-0.6
O ^d	4.24	0.48	10.07	6.4 (1.97)	6.9 (1.92)	-13.6	-1.4
P ^d	4.68	0.66	11.42	5.9 (2.01)	6.9 (1.96)	0.3	0.0
L	2.31	1.31	5.41	9.1 (1.87)	9.6 (1.83)	13.4	2.5
G	1.52	1.45	3.85	8.5 (2.02)	7.9 (2.05)	45.8	11.9
J	4.20	0.16	10.08	5.1 (2.00)	5.8 (2.08)	6.4	0.6
J	1.53	-0.49	7.23	4.8 (2.04)	5.6 (2.09)	1.0	1.3
J	4.04	2.20	18.95	6.3 (2.03)	6.3 (2.02)	0.3	0.4
		average		6.9	6.8		
		std.dev.		1.1	1.0		

^aDust mass penetrating the unenergized precipitator.^bNormalized dust mass penetration difference between the two precipitators.^cLognormal mass median aerodynamic diameter (w/geometric standard deviation) of dust penetrating the precipitator.^dSamples obtained from longwall run-of-mine material.

NOTE: Total pulverizing time for tests 1-6 was 90 s.

Total pulverizing time for tests 17-29 was 60 s.

Total pulverizing time for tests 30, 31 was 30 s.

TABLE 4. Dust mass and electrostatic charge generation characteristics of Pittsburgh coal.

Test	$M(u)^a$ mg	$M(u) - M(e)^b$ $= M(p)$ mg / mg / kg	Specific Dust mg / kg	Average Electric Field, E, Volts / cm	Average Specific Field, E _s , V / cm / mg / kg
1	0.45	1.25	0.88	2.4	2.7
2	0.05	-0.01	0.11	0.2	1.8
3	0.16	1.08	0.35	0.0	0.0
4	0.50	0.95	0.96	4.0	4.2
5	0.66	0.90	1.17	8.0	6.9
6	0.68	1.10	1.23	8.0	6.5
7	0.31	1.35	0.64	0.4	0.6
8	0.74	1.03	1.32	7.6	5.7
9	1.04	1.00	1.83	9.2	5.0
10	0.93	1.22	1.73	6.6	3.8
11	1.32	1.27	2.42	5.8	2.4
12	0.32	1.15	0.62	0.0	0.0
13	1.24	1.33	2.27	6.4	2.8
14	1.29	1.30	2.38	5.8	2.4
15	1.36	1.28	2.51	6.0	2.4
16	0.88	1.27	1.64	6.6	4.0
17	0.78	1.27	1.51	8.0	5.3
18	0.78	1.30	1.50	6.6	4.4
19	0.93	1.46	1.80	13.4	7.4
20	0.73	1.34	1.43	17.8	12.5
21	0.76	1.41	1.49	15.4	10.4
22	0.15	1.53	0.36	1.6	4.5
23	0.08	-0.01	0.19	0.8	4.3
24	0.05	2.39	0.15	0.4	2.7
25	0.05	1.53	0.14	0.6	4.2
26	0.87	1.23	1.52	19.6	12.9
27	0.64	1.27	1.14	27.2	23.9
28	0.25	0.18	0.42	34.0	81.7
29	0.86	1.62	1.84	30.2	16.4
30	0.86	1.52	1.79	23.2	13.0
31	0.82	1.60	1.71	29.0	16.9
32	0.77	1.50	1.63	25.8	15.8

^a Dust mass penetrating the unenergized precipitator.^b Normalized dust mass penetration difference between the two precipitators.

NOTE: Total pulverizing time for all tests was 90 s.

of the samples prior to testing. For the samples in Table 1, the humidification was maintained throughout the testing period. For the Pittsburgh seam samples shown in Table 2, sufficient material was successively riffled to obtain small samples of uniform consistency. Also for the Pittsburgh seam

samples, tests were run after the initial humidification and allowing the samples to dry naturally in the chamber. At test 22, the chamber was rehumidified and the drying process repeated for testing. As shown by the coefficient of variation (CV) indices in Table 2, uniform samples were ob-

tained with a significant variation in only the ADL moisture content achieved by humidification.

EXPERIMENTAL RESULTS

Test data on 16 bituminous coals was obtained by random selection of coal samples to be pulverized. Data generated from the Pittsburgh seam was not random in the sense that samples were pulverized after drying for successively longer time periods. The data presented in Tables 3 and 4 is reported with the following convention: $M(u)$ is the mass penetration of the unenergized ESP for the 3 min sampling period and therefore is proportional to the total airborne dust generated by the pulverizer. The quantity $M(u) - M(e) = M(p)$ is the mass penetration difference between the

unenergized and energized ESP's, normalized per unit of $M(u)$, per unit of pulverized material. This quantity will be proportional to the electrostatic charge on the sampled dust particles up to a critical value of the electric mobility μ_c . Particles with $\mu > \mu_c$ will be captured within the energized ESP. The specific dust is the total mass penetration $M(u)$ per unit of pulverized material. The average specific electrostatic field E_s is the average electrostatic field E generated per unit of pulverized material.

16 Bituminous Coals

Table 3 and Figures 2, 3, and 4 summarize the test results for the suite of coals tested. The samples which were obtained from longwall ROM coal are shown as the un-

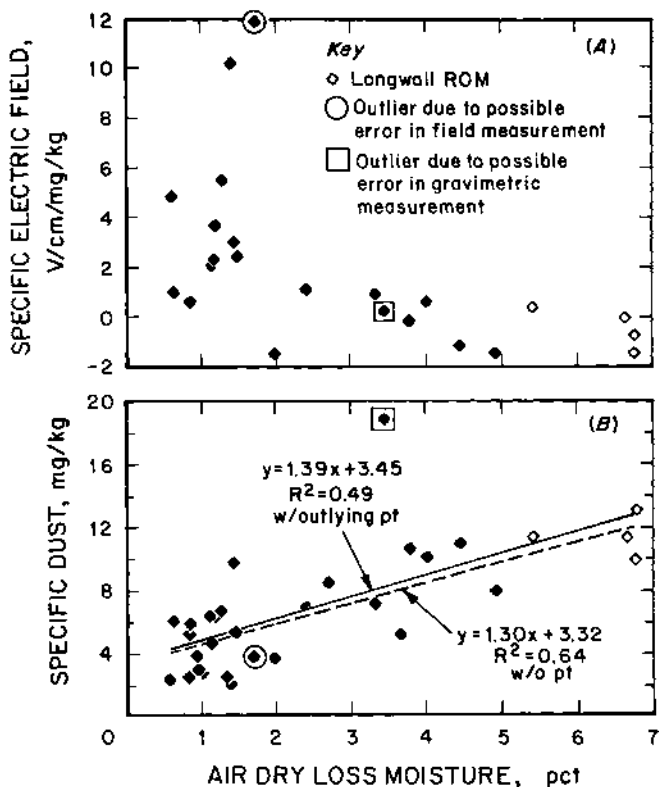


FIGURE 2. a) Specific electric field generated by 16 coal types as a function of ADL moisture, b) Specific dust generated by 16 coal types as a function of ADL moisture.

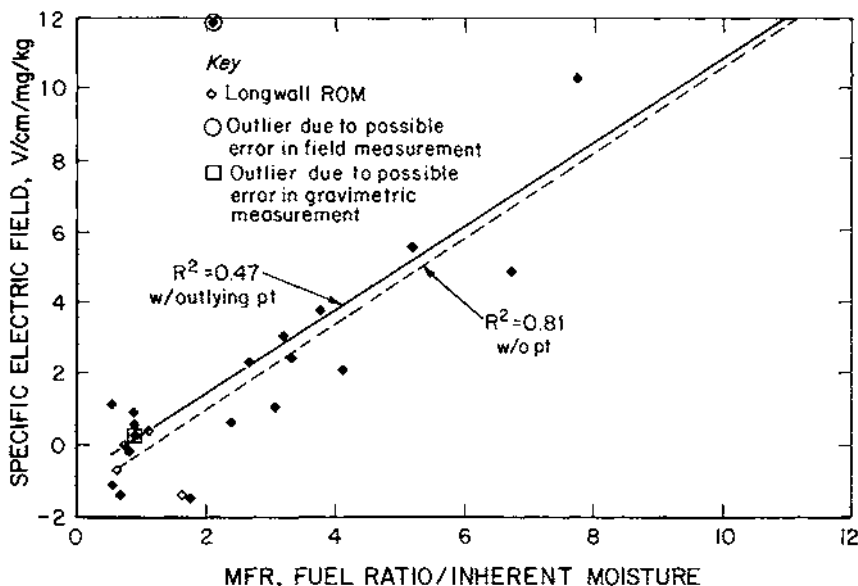


FIGURE 3. Specific electric field generated by 16 coal types as a function of the Moist Fuel Ratio (MFR).

filled points. It is noticed in Table 3 that a negative value is listed for $M(p)$ in test 30. This occurrence is most likely a weighing error in either $M(u)$ or $M(e)$ since it should not be possible for the condition $M(e) > M(u)$ to exist. Since this datum is not the outlying point for specific dust in Figure 2(b), the error may likely be in the value of $M(e)$. This point has, therefore, not been shown in Figure 4. Also in Table 3, measurements for E and E_s were not made for tests 1–7 and were lost due to data logger failure in test 17.

Figure 2(a) is a scatter plot of E_s vs the ADL moisture content of the coals. The notable feature of this plot is the sharp increase in E_s below an ADL value of approximately 2%, suggesting that these low moisture coals are in a highly charged state after comminution. Figure 2(b) plots the specific dust vs the ADL of the coals. The positive linear trend ($r^2=0.64$) is suggestive that there is significant agglomeration of dust particulate either in the bulk mate-

rial or in the airborne state of the low moisture coals. Comparison of Figures 2(a) and (b) suggests that the agglomeration is due to electrostatic charging of the coals rather than wetting and is in good agreement with larger scale crushing tests performed by Organiscak and Page (1998).

Since the ADL was significantly larger than the inherent moisture, it was believed that the ADL would be more influential on the electrostatic charging of the dust. However, scatter plots of both E_s and the specific dust vs the inherent moisture showed trends very similar to Figures 2(a) and (b) but with charge dissipation occurring at approximately 1% inherent moisture. Previous research had shown a negative exponential correlation between airborne dust and the inherent moist fuel ratio (IMFR) (Page et al. 1993). The IMFR is defined as the ratio of (fixed carbon ÷ volatile matter) ÷ inherent moisture and can be considered a measure of the coal rank. A similar trend between airborne dust and the IMFR was

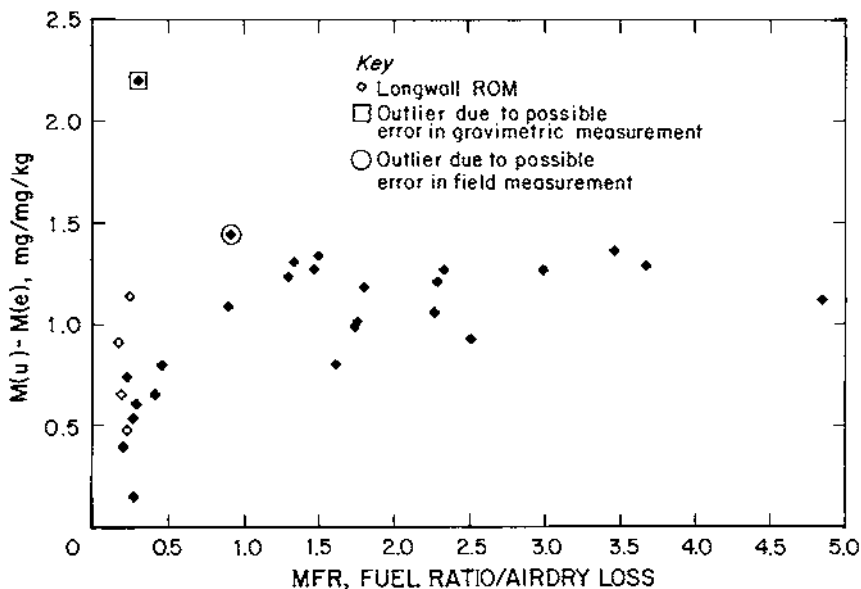


FIGURE 4. Gravimetric differential dust penetration of electrostatic precipitators for 16 coal types as a function of the MFR.

observed in this data set. Figure 3 plots E_s vs the IMFR and shows a positive linear correlation with an $r^2 = 0.81$ when excluding the singular outlying point.

Figure 4 plots $M(p)$ vs the MFR using the ADL moisture content. The plot shows that the lower rank, high moisture coals are in a low charge state, increasing positively with the ADL-MFR until the critical electric mobility of the dust particles is reached. A very similar trend was obtained with the IMFR.

Figures 2, 3, and 4 show two points which appear to be outliers in different circumstances. One point in each figure is circled and the other point in each is closed by a square. The uppermost point that is circled in Figure 2(a) may possibly be an outlier when Figure 3 is examined. However, no explanation is known for the extremely high field value. The uppermost point in 2(b), which is closed by a square, may be an outlier when Figure 4 is examined. An er-

ror in the gravimetric determination of $M(u)$ would cause such a deviation, although it is not known if this is the case. Since measurements of E_s and specific dust are independent, independently deviant points can be obtained between the plots. Regression lines and r-squared values for the linear plots of Figures 2(b) and 3 are shown which represent both the inclusion and exclusion of the apparent deviations.

Size distributions as measured with the impactors yielded efficient lognormal fits with adjusted r-squares ranging from 0.97 to 0.99 +. Analysis of the impactor data for all tests showed no difference in the mass median aerodynamic diameter (MMAD) or geometric standard deviation (GSD) of the dust distributions which penetrated either ESP. One ESP was not consistently higher or lower than the other ESP and the MMAD's for $M(u)$ and $M(e)$ were $6.9 \mu\text{m}$ (std. dev. = $\pm 1.1 \mu\text{m}$) and $6.8 \mu\text{m}$ (std. dev. = $\pm 1.0 \mu\text{m}$), respectively, as shown in

Table 3. In view of this result, it would appear that, over the size range of particles collected by the impactors, the particles were approximately equally charged within each test. Otherwise, it would be expected to see a shift in the MMAD and/or GSD of the dust penetrating the energized ESP since more highly charged particles would be preferentially captured by the ESP.

Pittsburgh Coal

Because of the similar relationships obtained between E_s and both the ADL and inherent moisture of the coal samples, another series of tests were run on humidified Pittsburgh seam coal prepared and tested as described above. Table 4 and Figure 5 summarize the test data for the Pittsburgh seam coal. It is noted that tests 2 and 23 have questionable negative values of $M(p)$

and are shown closed by a square and may possibly have erroneously low values of $M(u)$. Tests 24 and 25 used coal which was visibly moist and are shown circled in Figure 5.

Figure 5(a) shows the same trend as obtained in Figure 2(a) for the other coals tested but with a much more well-defined relationship of E_s with ADL. Undoubtedly, this results from eliminating other rank-related effects due to the fuel ratio and inherent moisture. Additionally, it would appear that the drier Pittsburgh coal is in a significantly higher charge state than the other coals tested. This may be more of an artifact than a real phenomenon for two reasons. First, it is noticed from Table 4 that test 28 produced only about one-third of the dust [$M(u) = 0.25$ mg] than the majority of other coals with an equivalent amount of ADL. No explanation is known

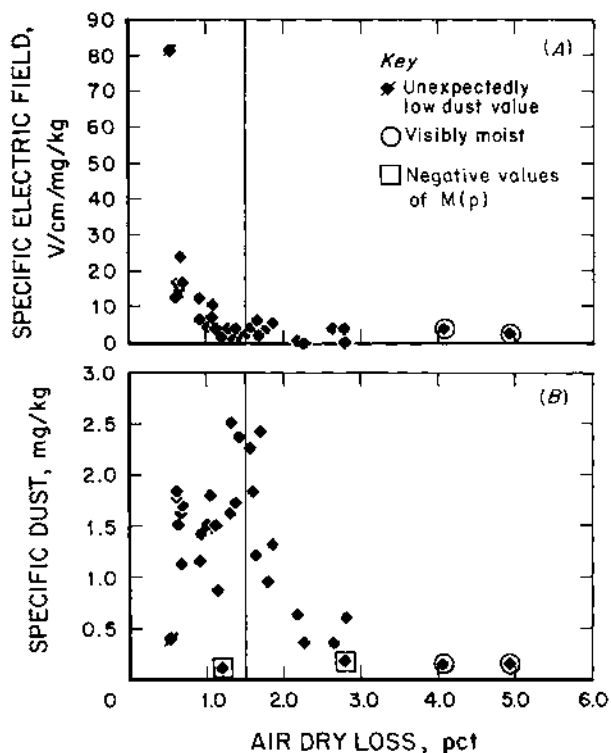


FIGURE 5. a) Specific electric field generated by Pittsburgh seam coal as a function of ADL moisture, b) Specific dust generated by Pittsburgh seam coal as a function of ADL moisture.

for this occurrence. Second, the DC offset voltage and amplifier gain values used to process the fieldmeter output were different for the two sets of data. This change in signal processing parameters was necessary to accommodate other testing being performed in the same time frame. Although the two sets of parameters were each adjusted to give proper calibration at the expected maxima and minima of the electrostatic field, small variations in offset voltage and amplifier gain could account for scaling differences. Nevertheless, each set of data is consistent within itself and illustrates the relationships of interest.

Figure 5(b) shows a remarkable feature which demonstrates competition between two dust-generation/liberation factors. It is observed that the specific dust generation appears to increase with ADL until approximately 1.5% ADL. This corresponds to a rapid decrease in E_s , at which point the net field has been reduced to a minimum. After 1.5% ADL the specific dust begins to decrease to a minimum at approximately 3% ADL. The two data points circled represent samples which were visibly moist.

It had been expected that tests on the Pittsburgh coal samples would remove some of the unexplained variation seen in the tests on the sixteen different coal seams. From Figure 5(b) it is apparent that there is still a significant amount of unexplained variation. Variations in fuel ratio and particle size distribution can be handily excluded. The most plausible source of this variation is in the varying time lag between the test and sample analyses. Although the samples were stored in sealed bags, the samples were not analyzed until as many as eight tests were performed. This corresponds to a time period of several weeks. As a result, there is a distinct possibility that the ADL moisture (which easily escapes the coal) was escaping the coal samples proportionally to the time between test

and analysis. This same systematic error would also be present in the tests performed on the sixteen different coal seams.

COMPARISON WITH UNDERGROUND COAL MINE DATA

For any given size distribution, agglomeration of respirable dust particles naturally produces an increase in the number of non-respirable particles with a simultaneous decrease in the number of respirable particles. If it is assumed that there exists a difference in agglomerating characteristics between coals of differing rank, it can reasonably be expected that this phenomenon would manifest itself in the percentage of respirable particles found in the 10 mm cyclone preseparator gritpot which collects the nonrespirable particles.

To investigate the effect of moisture content on the degree of particle agglomeration in underground coal mines, ARD samples were obtained from four longwall mining faces. Because a very large amount of coal must be collected to obtain an accurate estimate of the ADL moisture of coal after being mined (due to the addition of water by the mining machine water spray system) and the previous result that the inherent moisture content correlated with both E_s and the specific dust in a fashion similar to the ADL, the underground samples were examined for correlation with inherent moisture content.

For each face two ARD samples were taken at a fixed downwind distance from the shearer on each cut direction for two days, generating eight samples for each face. The respirable dust samplers used a 10 mm cyclone preseparator to remove the nonrespirable dust fraction, nominally $< 7 \mu\text{m}$, so that the gravimetric filter collects only the respirable dust which is considered to pose the greatest health hazard. The cyclone and

gritpot for each longwall sample was rinsed with isopropyl alcohol and the resultant suspension captured in a glass jar. To disperse any agglomerated particles, each suspension was prepared for size distribution by stirring for 5 min, then placing the sample container in a 200 W ultrasonic bath for 10 min, followed by restirring. Analysis of each sample was performed on a Horiba LA-500 particle size analyzer to yield 55 size intervals from 0.11 μm to 200 μm . For each size interval the percentage of particle sizes less than the stated size was calculated.

Underground Results

Table 5 shows the cyclone gritpot analysis for each ARD sample and the inherent moisture values for the bulk coal samples obtained at each mine. The numbers shown represent the percentages of particles < 6.72 μm captured by the cyclone. For consistency with the laboratory results, the underground test results were categorized for analysis according to inherent moisture < or > 1%. It can be seen that mine 1 has a significantly larger percentage of minus-6.72 μm particles than mines 2, 3, and 4 as well as the lowest inherent moisture content. Averaging these values, mines 2, 3, and 4 with > 1% inherent moisture have 19% of minus-6.72 μm particles in the gritpot compared to 30.8% for mine 1. Using the Student's t-test with 30 degrees of freedom for the difference in mean values, there is greater than 99.9% confidence that the mean values are different.

DISCUSSION OF RESULTS

ADL and Charge Effect

The laboratory pulverization tests suggest that coals with an ADL moisture content of approximately 1–2% or less which are

TABLE 5. Percentage of particles < 6.72 μm in cyclone gritpot of underground samples.

Mine	Day	% < 6.72 μm		Inherent moisture, %
		to tailgate	to headgate	
1	1	30.3	29.7	0.5
		29.6	23.6	
	2	30.0	32.6	
2	1	34.8	35.9	2.9
		21.1	20.2	
	2	17.6	36.0	
3	1	12.8	14.1	4.5
		12.9	18.4	
	2	22.7	18.9	
4	1	20.7	19.8	1.3
		22.9	9.9	
	2	21.4	16.3	
		19.4	15.0	
		24.3	18.1	
		21.8	15.8	
		21.7	14.4	
		$H_0 = \text{Mines 2, 3, 4}$		$H_1 = \text{Mine 1}$
		Average = 19.0		30.8
		std. dev. = 5.1		3.6
		Student's t-test statistics:		
		$t_{0.005} = 3.65$		
		$t_{\text{data}} = 6.42$		
		Conclusion = Reject $H_0 = H_1$		

freshly broken can be in a highly charged state, as observed from the electrostatic fields measured in this study. Although some coals may exhibit close to net neutral fields, particle charging can be significant. Other researchers (Polat et al. 1993), for example) have shown that there are almost equal numbers of positively and negatively charged particles for coals, resulting in a net neutral dust cloud. However, these results may be indicative of the process of redispersing dust as opposed to producing fresh airborne dust from comminution.

This research also suggests that the inherent moisture and ADL moisture content

of coal can have a significant effect on the amount of dust generated, the specific dust increasing due to less electrostatic agglomeration of the dust until the charge is neutralized. The electrostatic field could reflect the strength of fine dust attachment to large particles before airborne entrainment and/or reflect airborne agglomeration of small particles to larger particles, resulting in significantly more fallout before being sampled. After this point of charge neutralization, the ADL moisture begins to reduce the specific dust generated, possibly due to wetting agglomeration.

Although distinct trends are observed, there are not sufficient data to formulate a predictive model. However, a descriptive mathematical representation based on established physical laws is suggested. This mathematical representation involves the association observed between specific airborne total dust and ADL. From Figure 5(b), it is observed that the data could follow a set of serpentine-like curves having the functional form

$$y = abr^l / (a^m + r^m)^{n/2},$$

$$l = 0, 1, 2, 3, \dots \quad a, b = \text{constants}, \quad (1)$$

$$m = 2, 3, 4, \dots,$$

$$n = 1, 2, 3, \dots$$

The special case $l = 1, m = 2, n = 2$ is the *serpentine function*. Although it was studied and named by Sir Isaac Newton in 1701, the serpentine had been studied earlier by de L'Hôpital and Huygens in 1692. These serpentine-like functions have significant physical importance in that they recur frequently in solutions which describe gravitational and electrostatic fields. Due to the same inverse square law (differing only by constants) of both gravitational and electrostatic fields, these functional forms can be obtained for certain volumetric mass and charge distributions. As an example from elementary physics, the electrostatic field of an electric dipole has the electric

field E at points along the perpendicular bisector of the dipole axis (x) given by

$$E = 2aq / \left\{ 4\pi\epsilon_0 (a^2 + x^2)^{3/2} \right\} \quad (2)$$

$$(l = 0, m = 2, n = 3),$$

where ϵ_0 is the permittivity of free space, $2a$ is the charge separation, and q is the charge magnitude.

For distances where $x \gg a$, the essential properties of this charge distribution, defined as $2aq = p$, the electric dipole moment, enter only as a product. This means that if E is measured at various distances from the dipole, q and $2a$ can never be deduced separately but only as the product $2aq$. If q were doubled and a simultaneously halved, E at large distances from the dipole would not change. If the dust clouds generated by the pulverizer in these tests are considered to consist of particles of positive and negative charge (not necessarily equal in magnitude), then E may be considered to be a vector sum of many electric dipoles having distributions of a and q . The resultant field could have a serpentine-like functional form. It should be noted that l, m, n may not be restricted to integers for complex charge distributions.

In the presently described tests, E was measured at a fixed point with the generated dust cloud passing over the fixed measuring point as the dust was drawn out of the chamber for sampling. This is the equivalent of measuring E at various points r along the same direction of motion for a fixed dust cloud charge distribution in each test. Assuming varying degrees of charge state for the different coal samples crushed, the variations in E measured might be expected to have a form similar to

$$E \propto 2F(a)G(q) / \left\{ 4\pi\epsilon_0 (F^m(a) + r^m)^{n/2} \right\}, \quad (3)$$

where $F(a) = F(a\{\text{MFR}\}) = \text{some function which represents the dipole charge separa-}$

tions to be dependent on the airborne dust cloud concentration (higher concentrations imply smaller mean particle separation), presumed to be affected by the coal MFR; $G(q) = G(q\{ADL\})$ = some function which represents the dipole charge magnitude presumed to be affected by the coal ADL.

In fashion similar to the previously discussed characteristic of p , the same field can be obtained at a point for variations in q (*determined in large part by the ADL*) merely by adjusting r . Therefore, a serpentine-like functional relationship can reasonably be expected to exist between the specific dust generated and the charge-associated variable ADL, as shown in Figure 5(b). However, due to the complexity of the dynamic charge distribution, further investigations of additional coal seams and other parameters which may be significant are required.

Comparison of Figures 2(b) and 5(b) indicates that each coal may have its own characteristic charging and dust generation signatures. The suite of coals shown in Figure 2(b) show that specific dust generation still increases beyond 1.5% ADL content whereas the Pittsburgh seam coal shows a decrease in specific dust generation. A likely determining parameter would be the porosity of the coal and its ability to absorb moisture without appearing visibly moist or wet. None of the coals tested, except for Pittsburgh, showed any visible surface moisture up to nearly 7% ADL moisture.

Particle agglomeration is largely a result of electrostatic attraction of opposite electrostatic charges on the particle surfaces. During the breakage of materials, separation of electric charge occurs with the magnitude and sign of charge retained on each surface being functions of rate of separation and material work function. Because of the tremendous amount of energy expended and delivered to the coal material during mining, it is reasonable to expect

these dust particles to be initially in a highly charged state. In the absence of a charge neutralization mechanism, such as particle leakage paths, there are at least two scenarios which may occur. First, some particles may have such a high initial electrostatic charge that they become agglomerated in the product material and never become airborne—the percentage becoming airborne being a function of, among other factors, the degree of charging. Second, it is possible that some particles may retain significant amounts of electric charge for a short time interval after ejection from the breakage process. During this time, electrostatic agglomeration of particles would be observed due to the fact that coal dust aerosols are known to contain particles of positive and negative charge. However, it would be expected that the highest probability for agglomeration would occur immediately after ejection, where the particles are in closest proximity. At some distance from the point of ejection it would seem reasonable that additional particle agglomeration would no longer occur due to the large mean path length between particles. If it is assumed that particle surface leakage paths are correlated with the coal moisture content, then the expected result would be that low moisture coals would be in a higher state of agglomeration than high moisture coals. Although nonconclusive and lacking in quantity, the underground dust sampling data substantiates this hypothesis and is in agreement with the laboratory results which show the coals with less than approximately 1% inherent moisture content to be in a highly charged state after grinding.

Dust Control and Health Impacts

Coal mine worker health and dust control methods may likely be influenced by the coal properties discussed above. The amount of airborne dust generated affects

worker exposure and the type and level of dust controls used. Melandri found that lung deposition increased by up to 30% with charging properties of airborne dust (Melandri et al. 1983). Furthermore, Melandri suggested that the charge characteristics produced by breakage may carry a very large number of elementary charges and that the deposition efficiency may be greatly affected by the charge distribution. The increased prevalence of CWP observed with coal rank may be partly related to the direct correlation of increased lung deposition with dust cloud charging in higher ranked coals as seen in this research study.

Research on dust control with water additives (surfactants) to increase dust suppression have been conducted in the past with mixed and inconclusive results (Kost et al. 1981). Recent field research showed significant ARD reductions with anionic wetting agents added to the spray system of a longwall operation mining a higher ranked bituminous coal, while marginal ARD changes were measured with these surfactants applied at a longwall mining a lower ranked bituminous coal (Kilau et al. 1996). Laboratory research on water droplet charging with respect to concentration of cationic surfactants showed a strong correlation between water droplet charge and airborne coal dust capture (Polat et al. 1993). These research results suggest that worker health and dust control effectiveness may likely be influenced by airborne coal dust properties generated from freshly broken coal.

CONCLUSIONS

Results of these pulverizing experiments show that only coals below 1–2% ADL moisture content are in a highly charged state after pulverization and that the amount of charging decreases rapidly with increasing ADL up to 1–2%. This appears

to have a direct effect on the specific dust generation characteristics of coals. However, each coal may have its own characteristic dust charge and generation signature. Underground dust samples obtained in coal seams with inherent moisture contents ranging from 0.5 to 4.5% show that significant particle agglomeration exists for the 0.5% inherent moisture coal but not the coals with moisture > 1.3% inherent moisture, in agreement with the laboratory tests.

The author would like to thank Jay Colinet, John Organiscak, and Bud Spencer of the NIOSH Pittsburgh Research Laboratory Dust Control & Ventilation group for collecting the longwall run-of-mine bulk coal samples.

References

- American Society for Testing and Materials (1996). *ASTM D3172-Standard Practice for Proximate Analysis of Coal and Coke*, Annual Book of ASTM Standards: Volume 05.05, pp. 288–297.
- Attfield, M. D., and Moring, K. (1992). An Investigation into the Relationship Between Coal Pneumocoriosis and Dust Exposure in U.S. Coal Miners, *Am. Ind. Hyg. Assoc. J.* 53(8):486–492.
- Attfield, M. D., and Seixas, N. S. (1995). Prevalence of Pneumoconiosis and its Relationship in Dust Exposure in a Cohort of U.S. Bituminous Coal Miners and Ex-miners, *Am. Ind. Med.* 27:137–151.
- Attfield, M. D., and Wagner, G. (1992). Respiratory Disease in Coal Miners. In *Environmental and Occupational Medicine*, 2nd ed. edited by W. N. Rom. Little, Brown and Company, Boston, MA, pp. 325–344.
- Baafi, E. Y., and Ramani, R. V. (1979). Rank and Maceral Effects on Coal Dust. *Int. J. Rock Mech. and Min. Sci. (& Geomech Abstr.)* 16:107–115.
- Becker, R. S., Anderson, V. E., Allen, J. D., Birkhoff, R. D., and Ferrell, T. L. (1980). Electrical Image Deposition of Charges from Laminar Flow in Cylinders, *J. Aerosol Sci.* 1:461–466.
- Dodd, E. E. (1952). The Statistics of Liquid Spray and Dust Electrification by the Hopper and Laby Method, *J. Appl. Physics* 24:73–80.

- Hamilton, R. J., and Knight, G. (1957). *Laboratory Experiments on Dust Suppression with Broken Coal*, National Coal Board, Mining Research Establishment, Report No. 2083, 1957 Research Programme Reference No. 9.2.
- Hopper, V. D., and Laby, T. H. (1941). The Electronic Charge, *Proc. of Royal Society* 16:243–273.
- Hurley, J. F., and Maclaren, W. M. (1987). *Dust-Related Risks of Radiological Changes in Coal Miners over a 40-year Working Life: Report on Work Commissioned by NIOSH*, Edinburgh, Scotland: Institute of Occupational Medicine, Report No. TM/87/09.
- Johnston, A. M. (1983). A Semi-automatic Method for the Assessment of Electrical Charge Carried by Airborne Dust, *J. Aerosol Sci.* 14:643–655.
- Kaya, E., and Hogg, R. (1992). *In-situ Measurements of Agglomeration of Airborne Dust in Mines*, Emerging Process Technology for a Cleaner Environment. SME, Littleton, CO, 1992.
- Kilau, H. W., Lantto, O. L., Olson, K. S., Myren, T. A., and Voltz, J. I. (1996). *Suppression of Longwall Respirable Dust Using Conventional Water Sprays Inoculated with Surfactants and Polymers*, BuMines RI 9591, 53 pp.
- Knight, G. (1958). *The Formation of Dust and Debris and the Dispersion of Dust at the Breakage of Lump Coal in Relation to the Strength, the Water Content and Superficial Wetting*, London, U. K., National Coal Board, Mining Research Establishment Rpt. No. 2088, 1958 Research Programme Reference No. 9.2.
- Kost, J. A., Yingling, J. C., and Mondics, B. J. (1981). *Guidebook for Dust Control in Underground Mining*, Contact JO199046, Bituminous Coal Research, Inc., BuMines OFR 137-80, pp. 65–69; NTIS PB 81-130106.
- Kunkel, W. B. (1948). Growth of Charged Particles in Clouds, *J. Appl. Physics* 19:1053–1055.
- Kunkel, W. B. (1950). Charge Distribution in Coarse Aerosols as a Function of Time, *J. Appl. Physics* 21:833–837.
- Melandri, C., Tarroni, G., Podi, V., De Zaia-como, T., Formignani, M., and Lombardi, C. C. (1983). Deposition of Charged Particles in the Human Airway, *J. Aerosol Sci.* 15:657–669.
- Moore, M. P., and Bise, C. J. (1984). *The Relationship Between the Hardgrove Gindability Index and the Potential for Respirable Dust Generation*, Proc. of the Coal Mine Dust Conference Generic Technology Center for Respirable Dust, October 8–10, Morgantown, WV, pp. 250–255.
- National Institute for Occupational Safety and Health (1995) Criteria for a Recommended Standard: *Occupational Exposure to Respirable Coal Mine Dust*. DHHS (NIOSH) No. 95–106, September.
- Organiscak, J. A., and Page, S. J. (1998). *Investigation of Coal Properties and Airborne Respirable Dust Generation*, NIOSH RI 9645.
- Organiscak, J. A., Page, S. J., and Jankowski, R. A. (1992). *Relationship of Coal Seam Parameters and Airborne Respirable Dust at Longwalls*, BuMines RI 9425.
- Page, S. J., Organiscak, J. A., and Quattro, J. (1993). Coal Proximate Analysis Correlation with Airborne Respirable Dust, *Fuel* 7:965–970.
- Polat, M., Chander, S., and Hogg, R. (1991). *Characterization of Freshly Generated Airborne Dust of Quartz*, Proc. Int. Symp. On Respirable Dust in the Mineral Ind. Ed., R. L. Franz. Littleton, CO, pp. 267–274.
- Polat, H., Hu, Q., Polat, M., and Chander, S. (1993). *The Effect of Droplet and Particle Charge on Dust Suppression by Wetting Agents*, Pro. 6th U.S. Mine Ventilation Symposium, June 21–23, Salt Lake City, UT, Pub. SME, pp. 535–541.
- Stecklein, G. L., Branstetter, R., Arrowood, R., Davidson, D., Lankford J., Lyle, R., and Nulton, C. (1982). *Basic Research on Coal Fragmentation and Dust Entrainment*, Volume I-Technical Information (contract J0215009, Southwest Research Inst.). BuMines OFR 215(1)-83.
- Srikanth, R., Zhao, R., and Ramani, R. V. (1995). *Relationships Between Coal Properties and Respirable Dust Generation*, Proc. 7th U.S. Mine Ventilation Symposium, June 5–7, Lexington, KY, Pub. SME, pp. 301–309.
- U.S. Congress (1969). *Federal Coal Mine Health and Safety Act of 1969*, Public Law 91–1173.
- Yu, C. P., and Chandra, K. (1978). Deposition of Charged Particles from Laminar Flow in Rectangular and Cylindrical Channels by Image Force, *J. Aerosol Sci.* 9:175–180.

Received July 13, 1998; accepted October 11, 1999.